The Microstructural Mechanism on the Improvement of the Coercivity in 2 : 17-Type Samarium Cobalt Magnetic Compound

J. B. YANG, T. MOHRI, K. WATANABE
and K. ISHII

Abstract

The cellular precipitation microstructure of 2 : 17-type magnetic compound was studied at various states of aging by transmission electron microscopy. It was shown that, the initial supersatuated solid solution phase (1175°C, 50 hours) exerts a great influence on the precipitation behavior in the subsequent isothermal aging process. When the supersaturated phase was a $TbCu_7$-type disordered structure, it gives rise to a fine-scale continuous cellular precipitation microstructure which corresponds to a relatively high coercivity state. The cell interior is a Th_2Zn_{17}-type 2 : 17 phase which is separated by a thin continuous 1 : 5 boundary phase. On the other hand, when the supersaturated phase was Th_2Zn_{17}-type ordered structure, it only produces particle-like 1 : 5 phase precipitates along the large grain boundary of the Th_2Zn_{17}-type 2 : 17 phase, which corresponds to a very low coercivity state. An addition of copper stabilizes the $TbCu_7$-type disordered phase, and therefore increases the coercivity. The coercivity due to the fine-scale cellular precipitation microstructure in 2 : 17-type magnetic compound is found to be strongly dependent upon the coherency between the Th_2Zn_{17}-type cell interior and the 1 : 5 cell boundary phase. When the boundary interface was maintained in a coherent state, the coercivity increases steadily with the width of 1 : 5 cell boundary phase. However, when the coherency of the boundary interface is lost and the cellular precipitation microstructure breaks up, the coercivity falls rapidly.

1. Introduction

Since 1970, the 2 : 17-type Samarium-Cobalt intermetallic compound became a promising candidate as a permanent magnetic material[1)-5)]. This was mainly because there were some theoretical possibilities that could be reached to attain a very high magnetic property. However, attempts to develop high-quality magnets using the stoichiometric Sm_2Co_{17} compound were generally unsuccessful[6)], because the coercivity was very low. It soon became clear that, the addition of some alloying elements such as Cu, Fe, Zr, Mn, Cr etc. have remarkable effects on the improvement of the coercivity. Thus, instead of stoichiometric Sm_2Co_{17} composition, attention has been concentrated on a composition range with the general

Department of Metallurgical Engineering, Faculty of Engineering, Hokkaido University Sapporo 060 Japan

formula Sm ($Co_{bal.}$ $Fe_{0.22}$ $Cu_{0.08}$ $Zr_{0.01-0.03})_z$ where $7<z<9$ and bal. = balance[7)-9)]. In fact, in 1977, Ojima et al[10)] achieved achieved 30 MGO_e $(BH)_{max}$ with the composition Sm ($Co_{0.68}$ $Fe_{0.21}$ $Cu_{0.01}$) $_{7.4}$ and in 1981, the same group[11)] announced that it had achieved $(BH)_{max}$ = 33 MGO_e with Sm ($Co_{0.65}$ $Fe_{0.28}$ $Cu_{0.05}$ $Zr_{0.02}$) $_{7.7}$. Further improvement of the magnetic properties were attempted through a series of heat treatment which consists of a solid solution treatment (SST) followed by a isothermal aging or step-aging. And, an optimum SST temperature range of 1160-1180° C and isothermal aging temperature range of 800-850°C were proposed[12)-14)].

Transmission electron microscopies[15)-20)] for these multicomponent compounds have revealed a cellular precipitation microstructure which consists of a cell of rhombohedral Sm_2 $(Co, Fe)_{17}$ phase (structure type R3m) separated by a thin continuous hexagonal Sm $(Co, Cu)_5$ boundary phase (structure type P6/mmm). However, both the origin of this fine-scale cellular precipitation microstructure and the relationships between the structures and the coercivity are still not fully understood.

In order to provide a firm basis for designing material with optimum properties, it is deemed indispensable to establish microstructure-properties relationships.

The particular emphasis of the present paper is placed on synthetic observation of precipitation behavior by X-ray, TEM as well as optical microscope for three kinds of 2 : 17-type magnetic compounds at various stages of the heat treatment.

2. Experimental procedure

Three kinds of 2 : 17-type compounds, Sm_2Co_{17}, Sm_2 $(Co_{1-x}Cu_x)_{17}$ and Sm ($Co_{0.674}$ $Fe_{0.216}$ $Cu_{0.096}$ $Zr_{0.014}$) $_{7.55}$, were adopted for the present study. All compounds were prepared by arc-melting. In order to improve the homogeneity of specimens and the compounds were remelted five times. Also, an excess amount of Sm, approximately 5wt. %, was added to maintain the required composition[21)].

For each heat treatment, the specimens were wrapped in Ta foil and sealed in evacuated silica tubes to avoid the oxidation. Solid solution treatment (SST) was performed at 1175°C for 50 hours, then the specimens were quenched by water. Following the SST, a series of isothermal aging treatment were carried out at 850° C from 30 min. to 128 hours.

The temperature during heat treatments were controlled and monitored with a Pt-(Pt-Rh) thermocouple and a digital voltmeter.

The metallographic samples were prepared by the method devised for the present study. Following the final polishment with a 0.01 micrometer Al_2O_3 polishing liquid, the samples were etched using a solution of 100 ml H_2O, 8 g CrO_3 with an addition of 2 g Na_2SO_4.

Then, the samples were rinsed in hot water and reimmersed in 20% chromic acid to wash away the etching reaction products. Foil specimens for transmission electron microscopy were thinned down to 20 micrometer by mechanical grinding and were further thinned by ion micromilling.

The X-ray diffraction investigations were performed using the powder method with CoKα target and Fe filter. Two types of the samples were prepared for

magnetic measurement : One is a powder with an average particle size of 50 micrometer and the other is polymer-bonded powder which were pressed under 50 KOe pulse magnetic field so that a preferential spin alignment is achieved. The magnetic measurement were carried out using a vibrating samples magnetometer (VSM) under 15 KOe.

3. Results and discussions

The binary Sm_2Co_{17} and the multicomponent 2 : 17-type intermetallic compound have been reported to be crystallized into three modifications[22], ie. $TbCu_7$-type hexagonal phase, a Th_2Ni_{17}-type hexagonal phase and a Th_2Zn_{17}-type rhombohedral phase. Both the $TbCu_7$-type and Th_2Ni_{17}-type phase are a high-temperature phase, while Th_2Zn_{17}-type phase is a low-temperature phase. These three kinds of crystal structure, as shown in Fig. 1, can be derived from the $CaCu_5$-type $SmCo_5$ structure by a substitution of two small Co-atom dumbbell in place of one large Sm atom. If such substitution is random, it produces a $TbCu_7$-type disordered structure, while for ordered substitution, it produces either a Th_2Ni_{17}-type or a Th_2Zn_{17}-type structure depending upon the substitution sequence ABABAB …… or ABCABC……, respectively. Therefore, both the Th_2Ni_{17}-type and the Th_2Zn_{17}-type 2 : 17 phase are superlattice structures of the $TbCu_7$-type disordered phase.

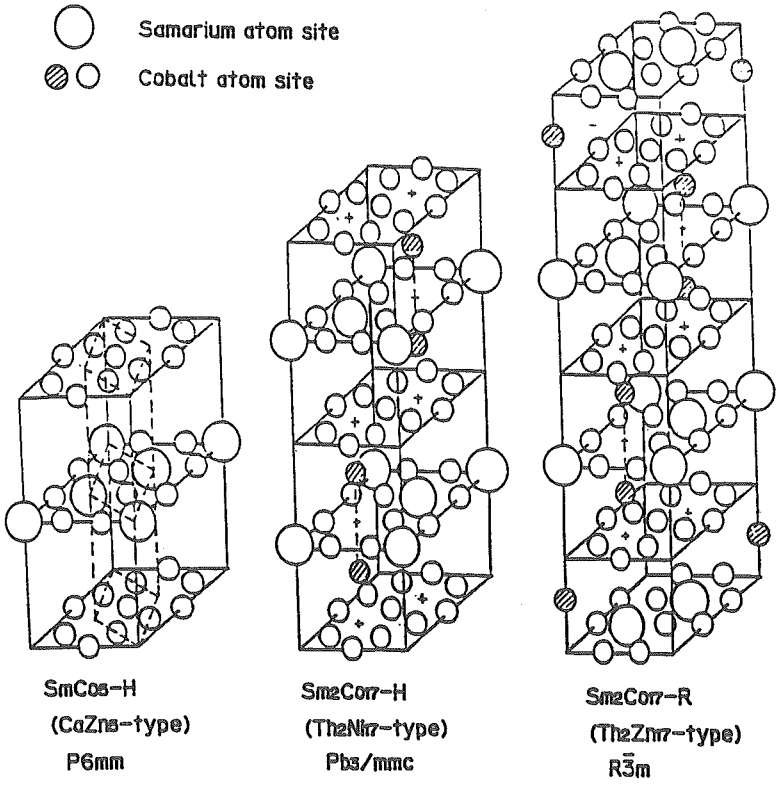

Fig. 1 Crystal structures in samarium-cobalt system.

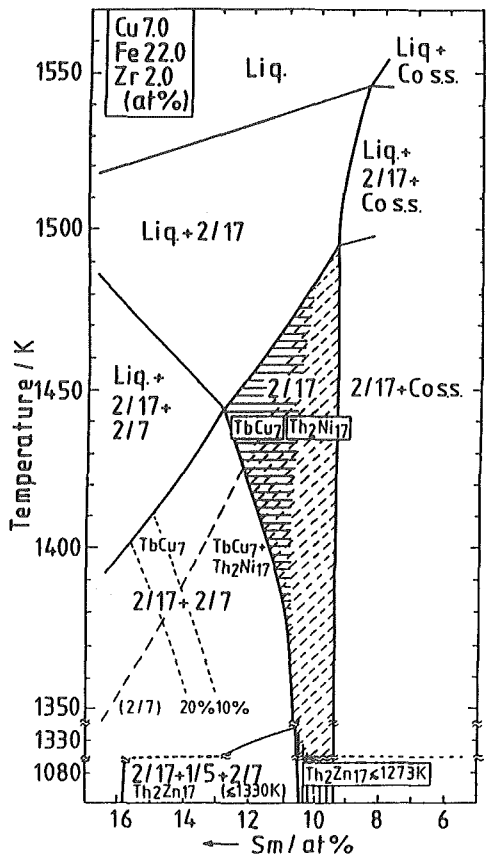

Fig. 2 A section of phase diagram in multicomponent Sm-Co7. 0 at.%Cu-22.0 at.%Fe-2.0 at.%Zr system[25].

The stability of each phase is influenced by an additive element as will be described in the following section.

3.1 X-ray diffraction study

X-ray diffraction pattern of Sm_2Co_{17} after arcmelting is demonstrated at the top of Fig. 3 which is characterized by $TbCu_7$-type disordered single phase. The as -cast samples in the other two groups, $Sm_2(Co_{1-x}Cu_x)_{17}$ and Sm_2 (Co, Fe, Cu, Zr)$_{17}$, are also consist of the single $TbCu_7$-type phase. The rest of X-ray the diffraction pattern in the Fig. 3 show phase transformation behavior in the course of SST and a series of isothermal aging treatment. At the SST, the Th_2Zn_{17}-type ordered phase is created, which is clearly identified by (024) characteristic peak. The obtained lattice constants are a = 8.396 A and c = 12.147 A. In the subsequent aging process at 850°C, no phase transformation are observed on the patterns, although variation of peak intensities is seen.

The X-ray diffraction pattern of SST stage at 1175°C for 50 hours are shown in Fig. 4 for the $Sm_2(Co_{1-x}Cu_x)_{17}$ with five different x values. Judging from the

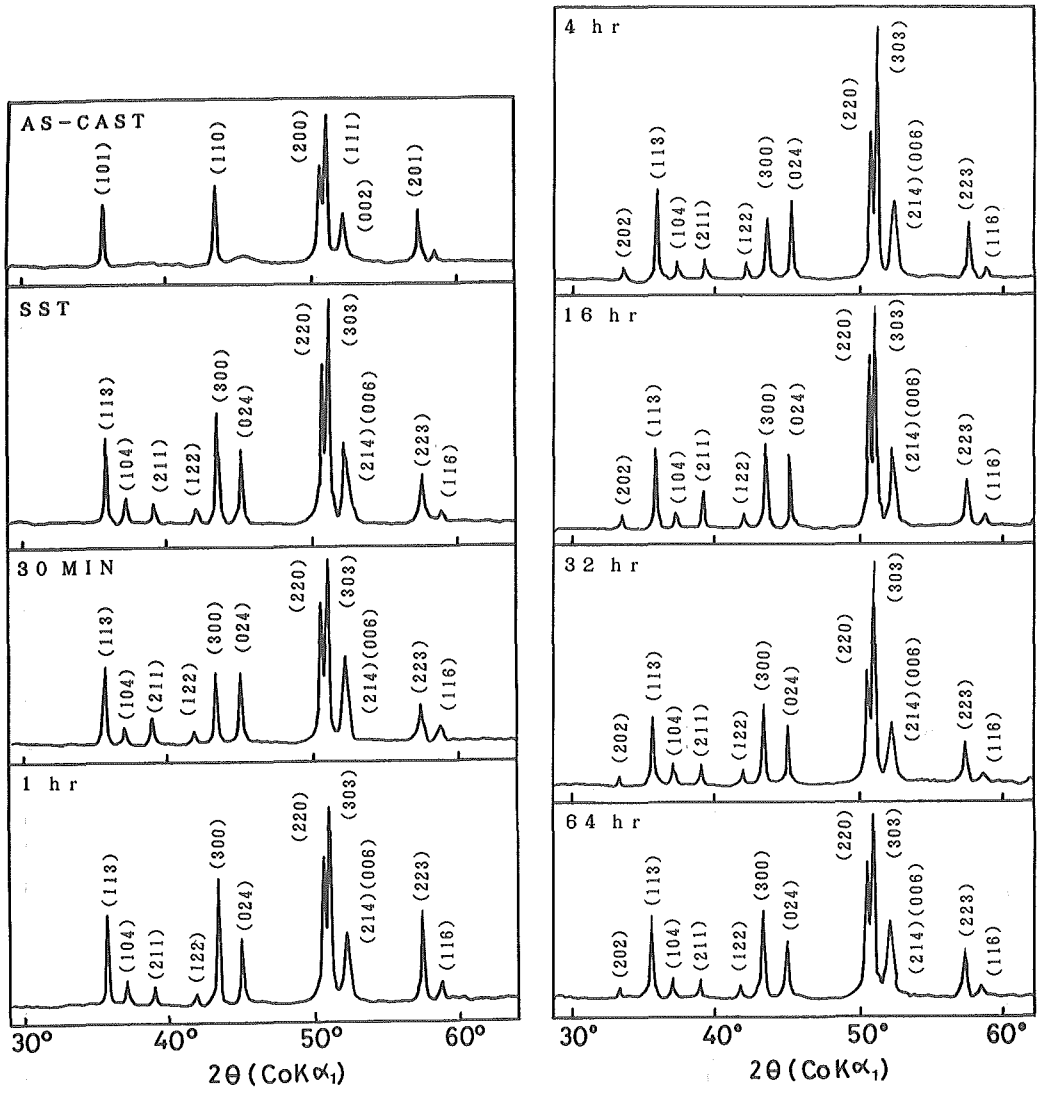

Fig. 3 X-ray diffraction patterns of Sm_2Co_{17} compound in the various heat treatment conditions.

distinct $K\alpha_1$ and $K\alpha_2$ peaks resolved in the higher Bragg angles, which is although not shown in this report, the phase is presumably in a supersaturated state. The stability of supersaturated phases at SST shows a strong dependence on the concentration of copper. When the copper concentration is small, the supersaturated phase tends to take a Th_2Zn_{17}-type structure. While for the higher concentration of copper (for example $x>0.2$), the supersaturated phase is transformed into the $TbCu_7$-type disordered phase, as is seen by the decaying of (024) peak. That is, the $TbCu_7$-type disordered phase is strongly stabilized by the addition of copper. Furthermore, when x value exceeds 0.3, the 1 : 5 phase is identified.

On the other hand, for a 2 : 17-type multicomponent magnetic compound Sm_2

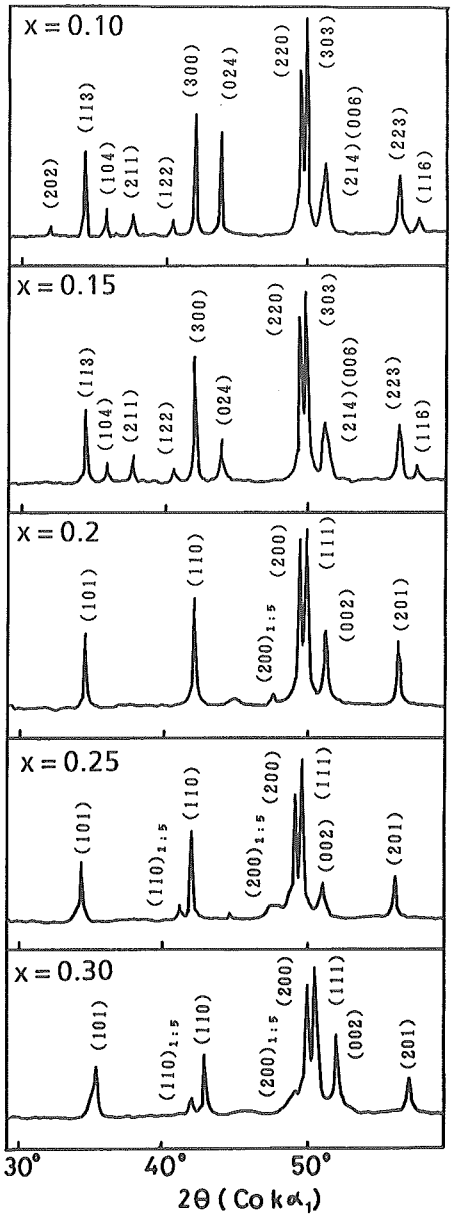

Fig. 4 X-ray diffraction patterns of $Sm_2(Co_{1-x}Cu_x)_{17}$ system with a series x values at solid solution treated states.

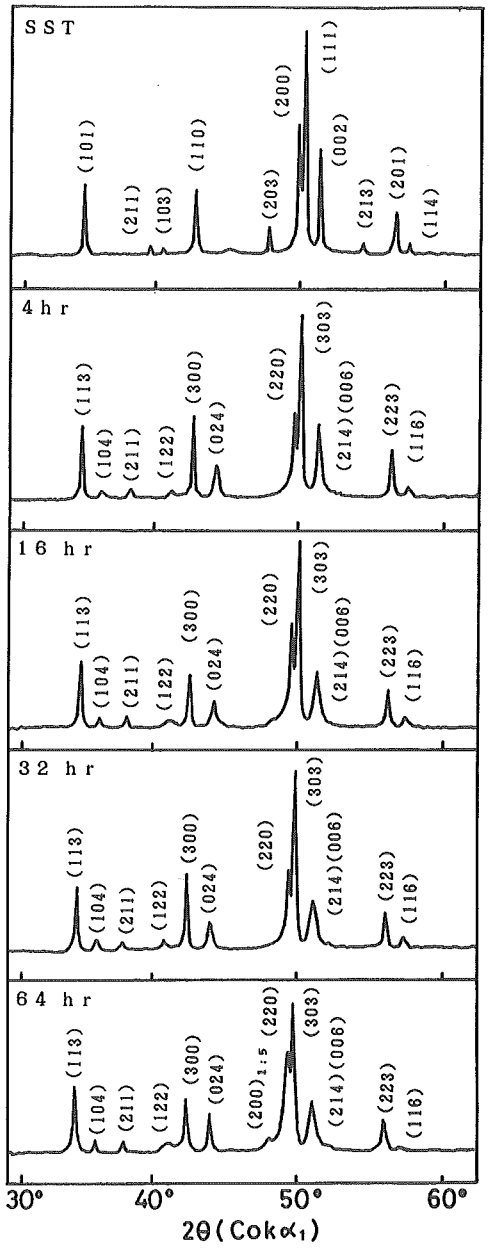

Fig. 5 X-ray diffraction patterns of Sm $(Co_{0.674}\ Fe_{0.216}\ Cu_{0.096}\ Zr_{0.014})_{7.55}$ at various states of heat treatment.

(Co, Fe, Cu, Zr)$_{17}$, the supersaturated phase at SST exhibits a $TbCu_7$-type disordered structure with the lattice constant a = 4.858 A and c = 4.100 A as is shown in Fig. 5. By the isothermal aging, the disordered $TbCu_7$-type supersaturated

Table 1. The summary of phase conditions at various states of heat treatment for three groups of samples.

	Sm_2Co_{17}	$Sm_2(Co_{1-x}Cu_x)_{17}$	$Sm_2(Co,Fe,Cu,Zr)_{17}$
As-cast	$TbCu_7$-type disordered	$TbCu_7$-type disordered	$TbCu_7$-type disordered
SST 1175℃ 50hr	Th_2Zn_{17}-type ordered	Th_2Zn_{17}-type → $TbCu_7$-type ordered → disordered	$TbCu_7$-type + small Th_2Ni_{17}-type disordered
Aging 850℃	Th_2Zn_{17}-type ordered		Th_2Zn_{17}-type ordered

phase decomposes into the ordered Th_2Zn_{17}-type phase and the 1 : 5 phase.

The changes of phase condition at various states of heat treatment are summarized in Table. 1. It should be reemphasized that the addition of copper strongly stabilizes the disordered $TbCu_7$-type 2 : 17 phase, and hence gives a great influence on the subsequent aging behavior.

3.2 The microstructures after isothermal aging

Fig. 6 shows the optical microstructure for Sm_2Co_{17} after isothermal aging at 850°C for various time lengths. Large particle-like precipitates along the grain boundaries are observed. It coarsens with the aging time, but no any precipitations are seen inside the grain. The precipitates exhibit a discontinuous distribution. The minimum size of the precipitates observed in the micrograph is larger than one micrometer. More detailed information has been provided by the electron microscopy. Fig. 7 shows the TEM micrograph after aging for 30 min. From the diffraction pattern, the precipitates along the grain boundary of 2 : 17 matrix were determined as the 1 : 5 phase. Also, a great number of twins are observed inside the 1 : 5 particles.

In contrast, the Sm_2 (Co, Fe, Cu, Zr)$_{17}$ compound shows a quite different precipitation behavior in the isothermal aging process at 850°C. Fig. 8 shows the optical microstructure after aging for various time. The precipitates exhibit a continuous morphology along the grain boundary, and coarsens with aging. It is

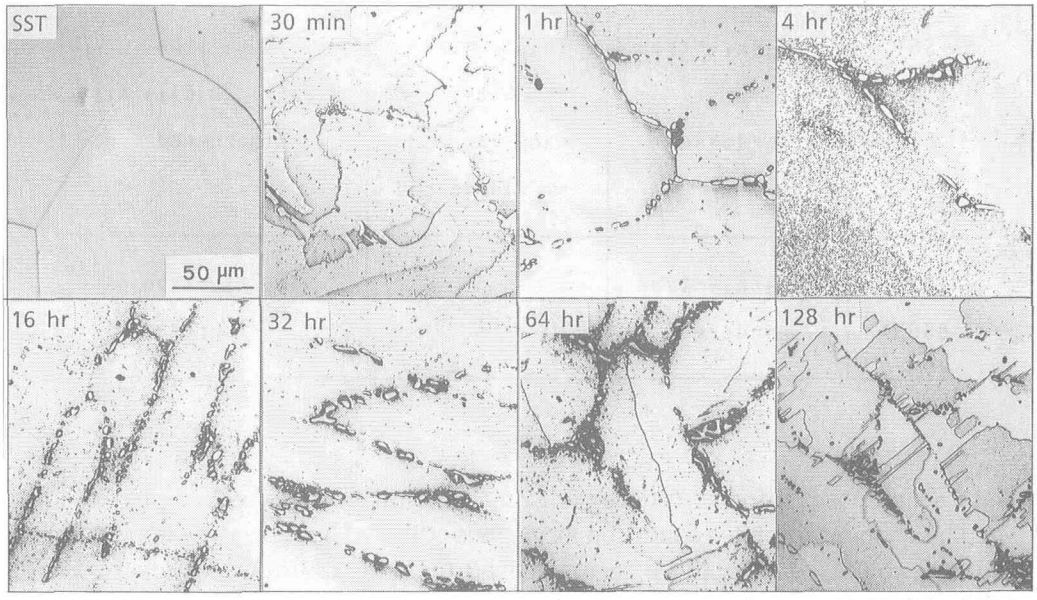

Fig. 6 Optical micrographs of Sm_2Co_{17} at a series of isothermally aged states at 850°C.

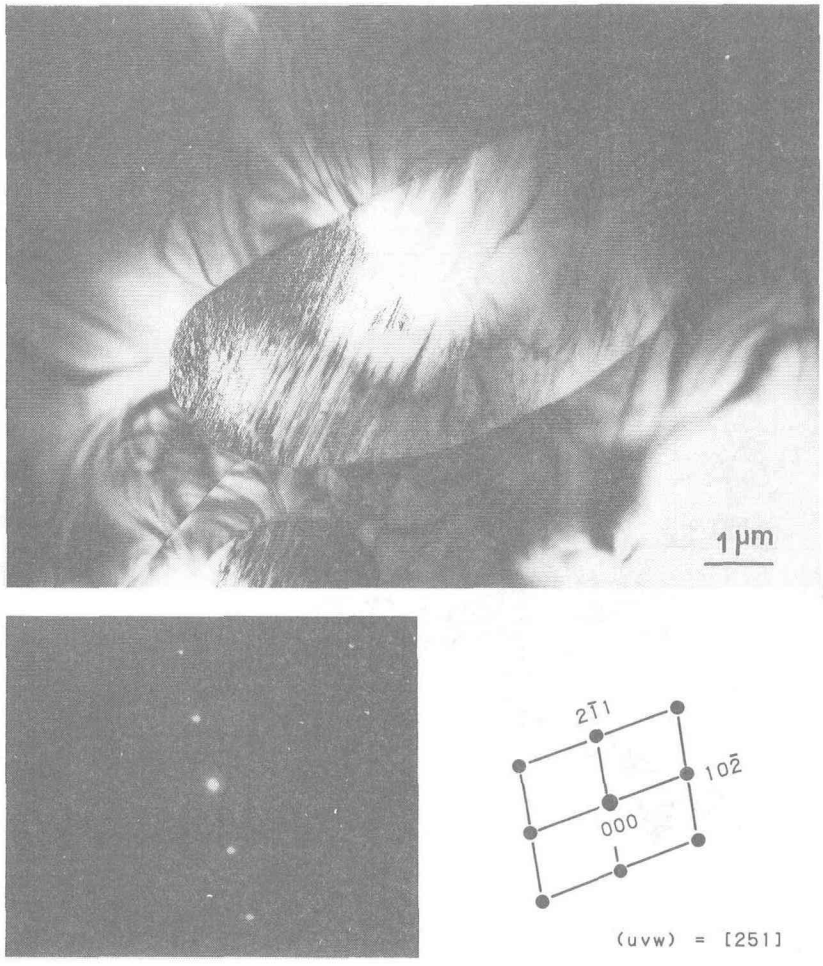

Fig. 7 Bright field electron micrograph near the $[251]_{1:5}$ beam direction after aging 30 min at 850°C.

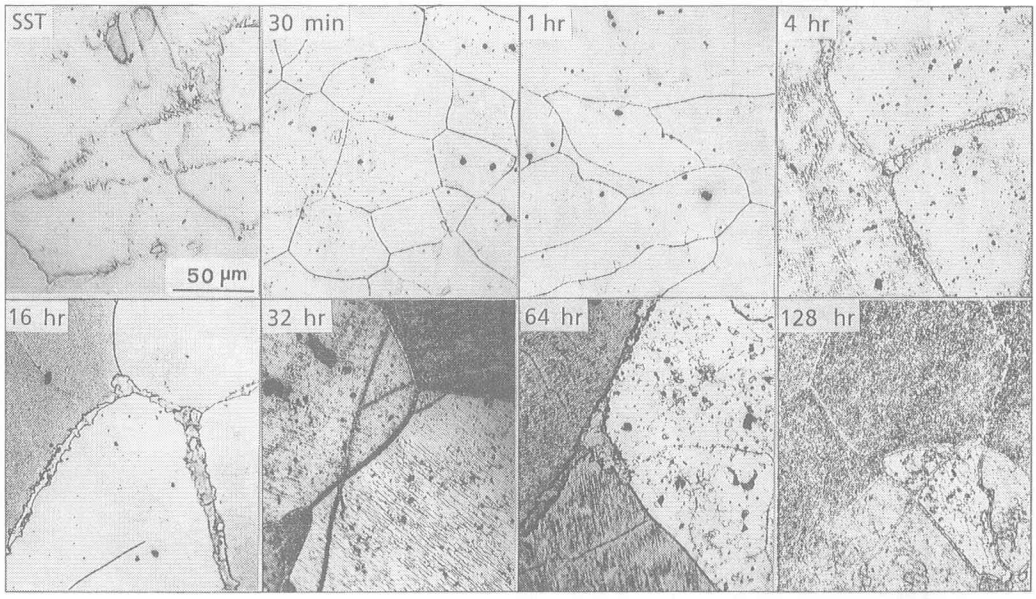

Fig. 8 Optical micrographs of Sm $(Co_{0.674}\ Fe_{0.216}\ Cu_{0.096}\ Zr_{0.014})_{7.55}$ at a series of isothermally aged states at 850° C.

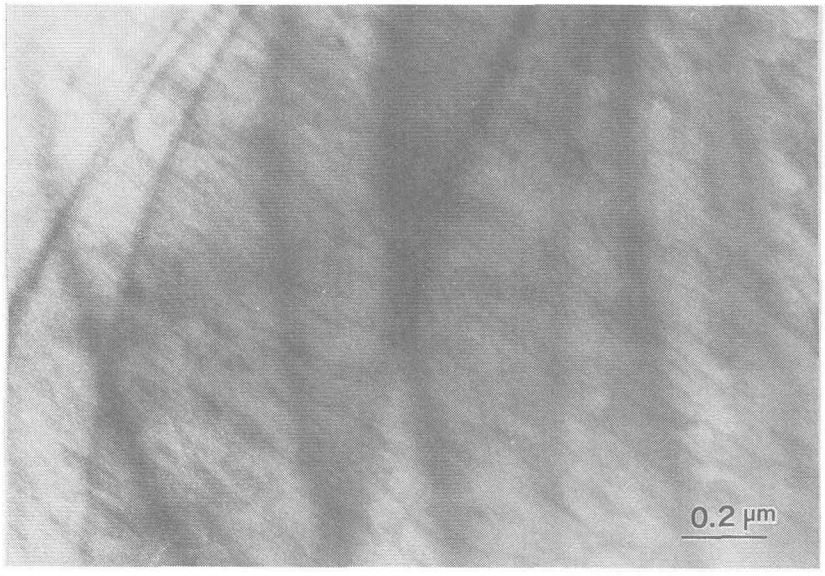

Fig. 9 Microstructure of solid solution treated Sm $(Co_{0.674}$ $Fe_{0.216}$ $Cu_{0.096}$ $Zr_{0.014})_{7.55}$ at 1175°C for 50 hours.

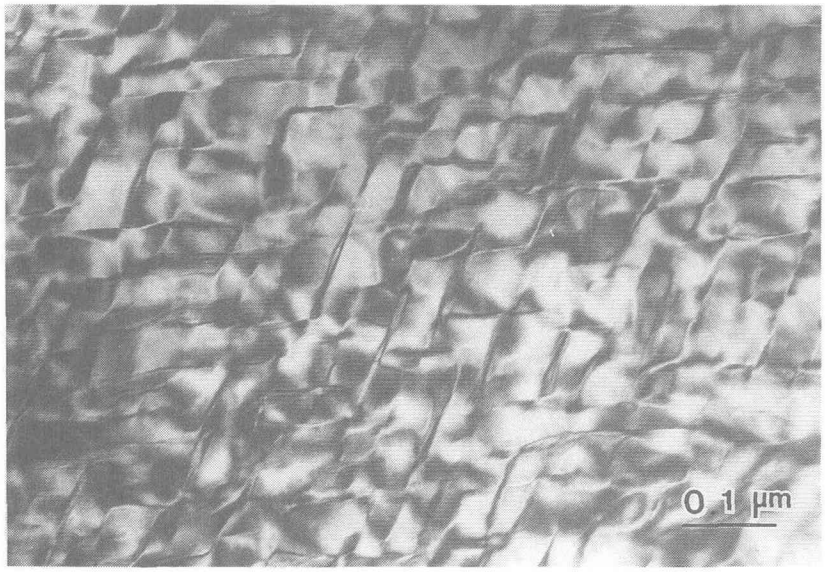

Fig. 10 Cellular precipitation microstructure of Sm $(Co_{0.674}$ $Fe_{0.216}$ $Cu_{0.096}$ $Zr_{0.014})_{7.55}$ aged 30 min at 850°C.

noticeable that, very fine and directional precipitates are formed inside the grain after 32 hours.

Immediately after the quenching from 1175°C, the micrograph shows a single $TbCu_7$-type phase in which only very fine phase separation is visible [see Fig. 9] .

Fig. 11 Cellular precipitation microstructure of Sm $(Co_{0.674}$ $Fe_{0.216}$ $Cu_{0.096}$ $Zr_{0.014})_{7.55}$ aged 32 hours at 850°C.

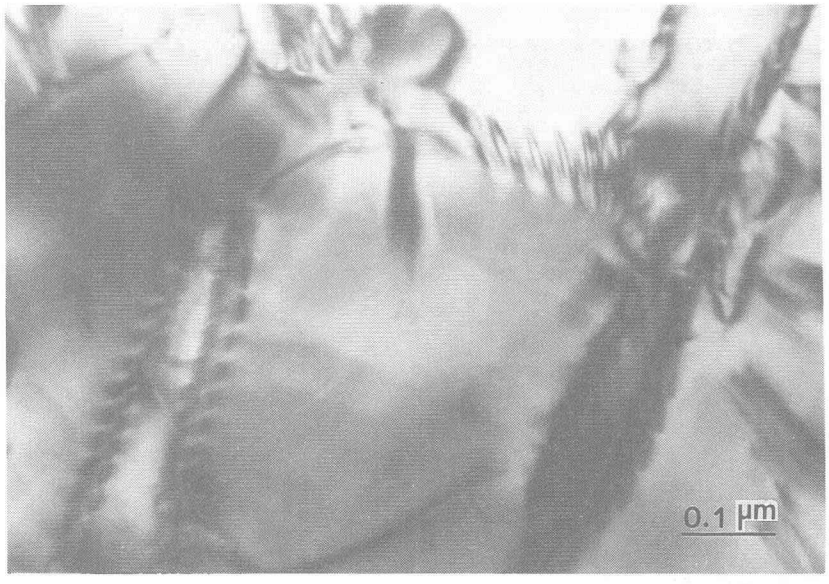

Fig. 12 Cellular precipitation microstructure of Sm $(Co_{0.674}$ $Fe_{0.216}$ $Cu_{0.096}$ $Zr_{0.014})_{7.55}$ aged 64 hours at 850°C.

Coercivity at this stage is, as shown in Fig. 13, only at the level of 400 Oe. At the initial stage of aging (30 min.) a coarser phase separation with an average size 500A in diameter is produced [see Fig. 10]. It can clearly be seen that the initiation of cellular microstructure commences at this stage. The cellular microstructure is coarsened as the aging process proceeds as demonstrated in Fig. 11, by which the

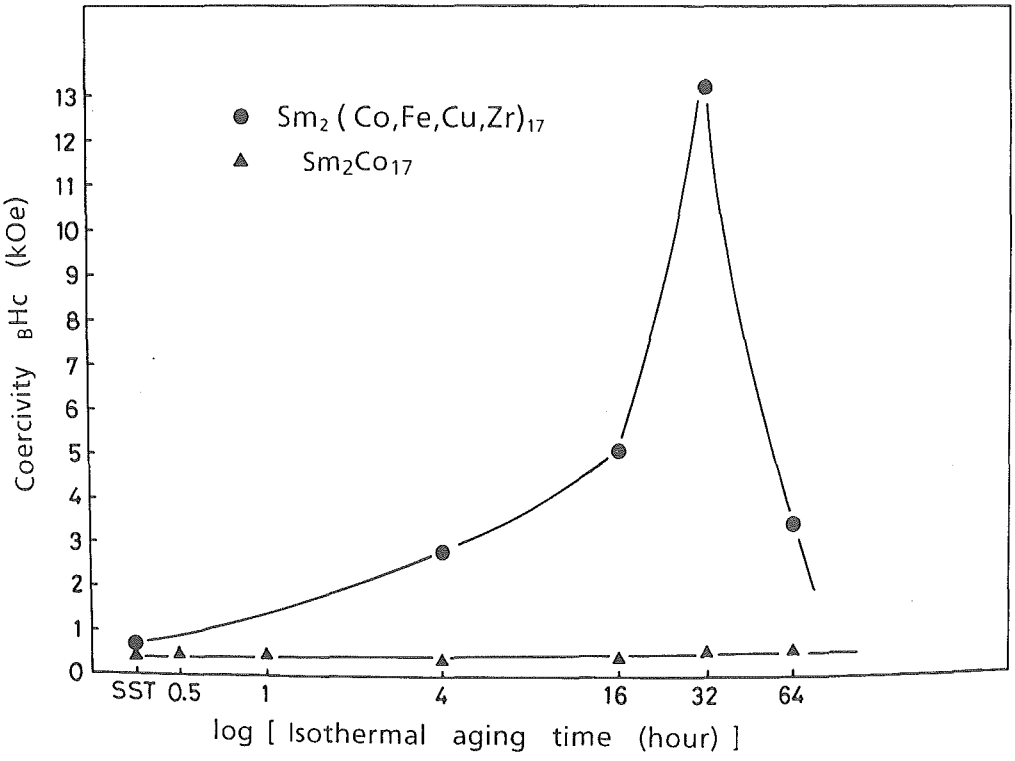

Fig. 13 The variations of the coercivity $_{B}Hc$ of Sm_2Co_{17} and Sm $(Co_{0.674}\ Fe_{0.216}\ Cu_{0.096}\ Zr_{0.014})_{7.55}$ as a function of the isothermal aging time.

coercivity data is strongly correlated.

Coercivity data [Fig. 13] show that up to the 16 hours the sample is at an underaged condition with coercivity less than 5.1 KOe. The coercivity reaches the peak value of 13.2 KOe after 32 hours which should be the optimum condition. Aging for 64 hours produced substantial overaging with a coercivity less than 2.7 KOe. The microstructure now shows a coarse semicoherent cell boundary interface with sets of parallel dislocations visible along the boundary interface, [see Fig. 12].

From the observation above, it is clear that, the higher coercivity state is related to the formation of a fine-scale cellular precipitation microstructure.

The present study further clarifies that, the formation of the cellular microstructure is determined by the supersaturated phase at SST stage (1175°C). When the supersaturated phase was a $TbCu_7$-type disordered structure, it gives rise to a finescale continuous cellular precipitation microstructure which corresponds to a relatively higher coercivity state. But when the supersaturated phase was Th_2Zn_{17} -type ordered structure, it only produces a macroscopic 1 : 5 precipitate particles

along the large grain boundary of the Th_2Zn_{17}-type 2 : 17 phase, which corresponds to a very low coercivity state. A comparison of the three groups samples clarifies that the copper addition strongly stabilizes the $TbCu_7$-type disordered phase and therefore increases the coercivity. For the fine-scale cellular microstructure, the domain wall pinning as due to difference of the magnetic anisotropy and magnetic exchange interaction between the cell interior and cell boundary. At a demagnetized state, the domain wall is pinned within a cell. The strength of the pinning force is determined by the width of boundary region and the internal stress. When the boundary interface held coherent, the internal stress near the boundary region is also high, thus it gives rise to a strong pinning to the migration of domain wall and, hence, enhances the coercivity. When the coherency of the cell boundary is lost, the internal stress is decreased by introducing a set of parallel interface dislocations. Consequently the pinning interaction is weakened and hence the coercivity decreased. A more detailed quantitative discussion will be presented in a forthcoming publication.

Acknowledgments

The authors are grateful to Mr. Hara et al (Mitsubisi Steel Co.) for their kind help for the measurement of magnetic properties. And particular thanks are due to Mr. K. Okubo who provided much help in certain parts of the experiment.

REFERENCES

1. J. J. Becker ; J. Appl. Phys 41 (1979) p. 1055.
2. M. G. Benz and D. L. Martin ; Appl. Phys. Lett. 17 (1970) p. 176.
3. F. F. Westendorp ; IEEE Trans. Magn. MAG-6.
4. O. A. W. Strydom and C. Alberts ; J. Less-Common. Metals 22 (1970) p. 503.
5. H. Zijlstra ; J. Appl. Phys 41 (1970) p. 4881.
6. M. Merches, W. E. Wallace and R. S. Craig ; J. Magn. Magn. Mater. 24 (1981) p. 97.
7. C. Sochen, W. Run, C. Chengyi, H. Yaofu ; Proceedings of the 5th International Workshop on RE-Co, P. M. and their Applications. Paper No. IX-3 (1981) p. 459.
8. T. D. Sun ; Proceedings of the 6th International Workshop on RE-Co P. M.and their Applications. Paper No. PIV-7 (1982) p. 433.
9. A. Kianvash, I. R. Harris ; J. Mater. Sci. 19 (1984) p. 353.
10. T. Ojima, S. Tomizawa, T. Yoneyama and T. Hori ; IEEE Trans. Magn. MAG-13 (1977) p. 1317.
11. R. K. Mishra, G. Thomas, T. Yoneyama, A. Fukuno and T. Ojima ; J. Appl. Phys. 52 (1981) p. 2517.
12. A. Kianvash and I. R. Harris ; J. Less-Common. Metals 98 (1984) p. 93.
13. T. Yoneyama, S. Tomizawa, T. Hori and T. Ojima ; Proceedings of the 3rd International Workshop on RE-Co P. M. and their Applications. Paper No. VII-1 (1978) p. 406.
14. C. Sochen, W. Run, C. Chengyi, H. Yaofu and S. Guangfei ; Proceedings of thce 5th International Workshop on RE-Co P. M. and their Applications. Paper No. IX-3 (1981) p. 459.
15. Raja K. Mishra and G. Thomas ; J. Appl. Phys 49 (3), March, 1978.
16. J. Fidler ; J. Magn. Magn. Mater. 27 (1082) p. 127.
17. J. Fidler ; IEEE Trans. Magn. MAG-19 No. 5 September, 1983.
18. F. Pothwarf, Y. Tawara, Ken Ohashi, J. Fidler, P. Skalicky, R. Grossinger and H. Kirchmayr ; Proceedings of the 6th International Workshop on RE-Co P. M. and their Applications. Paper No. S

-6.

19. R. J. Cremer, G. W. Reppel ; Proceedings of the 6th International Workshop on RE-Co P. M. and their Applications. Paper No. PIV-1.
20. C. George and Haijipanayis ; Proceedings of the 6th International Workshop on RE-Co P. M. and their Applications. Paper No. S-9.
21. G. Schneider, E. -TH. Henig, H. L. Lukas and G. Petzow ; J. Less-Common. Metals 110 (1985) p. 160.
22. Y. Khan ; Acta. Cryst. (1973) B29, p. 2502.
23. A. E. Ray ; J. Appl. Phys. 55 (6), 15, March, 1984, p. 2094.
24. Y. Morita, T. Umeda, Y. Kimura ; J. Japan. Inst. Metals. Vol. 52, No. 2 (1988) p. 245, in Japanese.